

Experimental Study of Near Field Regions of n-Heptane Spray

C. S. Vegad*, D. Ferrando, S. Idlahcen, A. Vandell, B. Renou, G. Godard, G. Cabot,
J. B. Blaisot, B. Duret, J. Reveillon, F. X. Demoulin

CORIA-UMR 6614, Normandie University, CNRS-University and INSA of Rouen, Avenue de
l'Université, BP 12, Saint-Étienne-du-Rouvray 76800, France

*Corresponding author: vegadc@coria.fr

Abstract

This paper measures spray quantities in continuous and dispersed regions of atomizing n-heptane conical liquid sheet. An industrial pressure swirl hollow cone spray injector is used to atomize n-heptane. A non-swirling co-flow air is supplied externally around the injector using an atmospheric CORIA Rouen spray burner (CRSB). The overall spray behavior is characterized by microscopic shadowgraphy imaging, while the optically dense regions are studied using the laser-induced fluorescence (LIF) technique. High contrast images of LIF facilitated the determination of contours of ligaments, liquid blobs, and other near-field liquid structures. A new post-processing technique is then implemented to predict the droplet diameter from the integrated length of all the contours. The phase Doppler anemometry (PDA) measurements are also carried out in the dispersed zone to validate the predicted droplet diameter. Results showed a decent agreement between estimated and measured diameters. The proposed method utilizing near-field information for an initial guess of droplet diameter is expected to be simpler, faster, and less expensive than the other postprocessing tools.

Keywords

LIF, n-heptane spray, PDA, droplet size prediction

Introduction

Atomized droplets are an influential parameter in reacting and non-reacting processes. A sequence of complex phenomena produces a wide range of droplets. These phenomena evolve spatiotemporally in the near-field regions, where a primary breakup is taking place in the gaseous medium. Such near-field regions carry footprints concerning the formation of the final droplets. In other words, an early stage of the atomization process significantly impacts the dispersed phase. The current attempt is a step toward understanding such a physical process by measuring the hollow cone spray near the nozzle using state-of-the-art experimental techniques.

Multiple approaches have been carried out to image the dense sprays. However, not a single method is available through which the entire spray can be described. The choice of diagnostic technique is based on the region under investigation. The spatiotemporal evaluation of dense flow can be imaged by employing the microscopic shadowgraphy using a flash lamp, or laser light source [1]. This may help explain the dynamic process. Since shadowgraphy is line-of-sight imaging, the images contain an out-of-focus spray regime. Thus, postprocessing results may also collect unwanted information. There are laser imaging techniques available to analyze two-phase flows by achieving high-contrast images. For example, the liquid core surrounded by a dense field of droplets can be captured by ballistic imaging [2–4].

When the laser-illuminated detection technique, i.e., Mie scattering, is applied to a dense spray, it may add non-physical spray information regarding artifacts in the final images. For partially atomized spray in the near nozzle field, the direct reflection of incident laser light at the liquid-air interface of non-spherical structures creates signal intensities strong enough to saturate the camera sensor. However, this is not the case for a fully atomized dispersed zone. Sometimes, the blurring effect due to multiple scattering in the central spray regions may reduce visibility.

One of the potential methods to minimize multiple scattering is by structured illumination [5–7]. In this technique, a spatially modulated laser sheet intensity is used to differentiate direct and multiple scattering.

Unlike Mie detection, laser-induced fluorescence (LIF) detection provides high-contrast images of dense spray. LIF detection is recommended for detailed analysis of ligaments, droplets, and other liquid structures present at the beginning of the atomization process [8]. In LIF, the collected signals are from the liquid bodies and their interfaces, thus representing their volume. Further, the LIF is much simpler [9] as compared to complex and costly X-ray imaging that uses a high-intensity synchrotron source to capture initial spray [10–12]. A review of different techniques to image principal spray regions is given in [13] and that for dense zones refer [14, 15]. When it is about the imaging of dense spray at the outlet of the injector, high contrast fluorescence images can be achieved by implementing the two-photon laser-induced fluorescence (2p-LIF) technique [16]. First of all, it is useful in the mitigation of multiple light scattering and also reduces the amount of collection of scattered light. The theory of two-photon absorption is available in [17, 18]. 2p-LIF is found to be more accurate to study spray structures [16, 19, 20]. The primary objective of the current study is to capture the continuous and atomized n-heptane hollow cone sheet at its initial stage. The challenge is to find a spray diagnostic technique that can mitigate the issues of near-field imaging. One of the promising techniques, based on the literature, utilized in the present analysis is 2p-LIF. The high contrast 2p-LIF images are post-processed by curvature analysis for the initial guess of droplet diameter. Further, the droplet diameter obtained from the new postprocessing technique is compared with those obtained by PDA measurements.

Experimental Setup

The experimental test facility is schematically presented in Fig. 1. In the present study, the CORIA Rouen spray burner (CRSB) was adopted to carry out n-heptane atomization process. CRSB consists fuel injection system and plenum. The fuel injector is located at the top of the injection system and opens into the chamber (Fig. 1). Injector is surrounded by a co-flow air stream guided through a convergent annular passage. The outer and inner diameters of the annular passage at the downstream end are 20 mm and 10 mm, respectively. While the upstream end is connected to the plenum that houses 18 radial vanes of zero-degree angle. The supplied air passes through the plenum, is directed towards the radial vanes and enters the chamber. The purpose of providing radial vanes is to break large flow structures. Further details on burner geometry are available in [21, 22].

A cylindrical coordinate system is considered here. In Fig. 1, Z and R represent the axial and radial spray directions, respectively. The spray formation is in the downward (positive Z) direction. An industrial pressurized swirl injector (Danfoss make) of 80° hollow cone and 1.35 kg h^{-1} flow rate was used to atomize n-heptane fuel. The injector orifice diameter is $200 \mu\text{m}$. The internal geometry of the injector is such that a portion of fuel pressure is utilized to form a rotating liquid film leading towards the orifice. While the remaining portion of fuel pressure is applied to force the liquid through an orifice as a conical sheet into the chamber. The chamber has a glass window fitted on each of the four sides. The chamber end faces the exhaust system to remove the fully atomized spray and thus avoid fogging within the chamber. In this way, and with co-flow air, liquid film formation on chamber walls can be avoided.

For all the experiments, n-heptane and co-flow air mass flow rates are 6 g s^{-1} and 0.28 g s^{-1} , respectively. N-heptane mass flow rate was regulated by Coriolis mass flow controller (Bronkhorst, CORI-FLOW, $0\text{--}2 \text{ g s}^{-1}$). A thermal mass flow controller (Bronkhorst, EL-FLOW, $0\text{--}15 \text{ g s}^{-1}$) controlled the air mass flow rate. The K-type thermocouples were used to measure n-heptane (T1) and air (T2) temperatures. Their injection pressures were measured using the PT1 and PT2 pressure transducers (see Fig. 1).

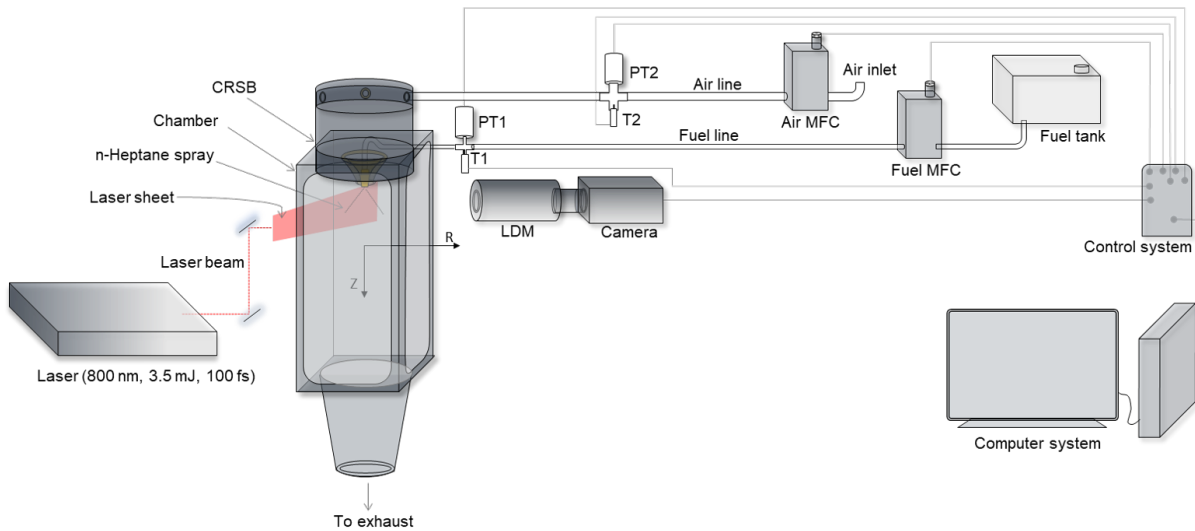


Figure 1. Schematic of the experimental setup demonstrating the instruments and optics arrangement for the 2p-LIF technique. The position of transmitter and receiver probes of PDA correspond to spray are shown. In the figure— 1 and 2 refers n-heptane and air; MFC, mass flow controller; T, thermocouple; PT, pressure transducer; Z and R represent axial and radial directions.

Optical Diagnostics

Experiments were begun with microscopic shadowgraphy to image an early stage of n-heptane spray. This technique is constructed based on the variation in light intensity arising from the deflection of rays while passing through the gradient under investigation. The deflection from the original path is due to the non-uniform refractive index of the media. Imaging was carried out at 25 kHz to capture the n-heptane hollow cone spray from the nozzle orifice to droplet formation zones. Since the primary breakup is within a 1.5 mm axial distance, it is recommended to use a microscope [9]. This was accomplished by using a long-distance microscope (LDM, QM-100, Questar) with a CMOS camera (1280×800 pixel² resolution, Phantom V2512). The complete imaging was within 5.32×3.33 mm² field of view at $4.16 \mu\text{m}$ per pixel optical magnification. Flow structures captured by shadowgraphy are seen to be accompanied by out-of-focus (blurred) regions as the current spray is highly dense. Thus, shadowgraphy could not provide clear insights into near-field regions because they contained unwanted information. The recommended technique for high contrast imaging of dense sprays is laser-induced fluorescence (LIF) [8]. LIF could meet the primary objective of the present study, which is to capture the events of n-heptane spray at its early stage and analyze them to predict the final droplet size. The current analysis employed two-photon laser-induced fluorescent (2p-LIF) technique to characterize the primary atomization of n-heptane spray. The reason for choosing 2p-LIF is explained in the next section.

An optical arrangement for 2p-LIF is shown in Fig. 1. The laser system used with this technique was 800 nm wavelength, 1 kHz, $3.5 \text{ mJ pulse}^{-1}$, 100 fs, regenerative amplified Ti:Sapphire (Coherent Inc.). The laser beam exhibits a 5 mm full width at half maximum (FWHM) Gaussian profile [5]. A cylindrical lens was employed to form a $\sim 200 \mu\text{m}$ thin laser sheet illuminating fuel-tracer solution spray. In this paper, pyromethene-567 is the tracer for n-heptane fuel. The choice of tracer is explained next. After absorption, the excited tracer molecules jump to higher energy states and decay to lower states by emitting fluorescent photons. An ICCD camera (PiMAX 4, 1024×1024 pixels²) was orthogonally positioned to collect fluoresced light (emission) from the spray. The peak emission ($\lambda_{max,fl} \sim 571 \text{ nm}$) was captured using a filter of center wavelength $565 \pm 24 \text{ nm}$ and 24 nm band width (MF565-24, Thorlabs). An excitation wavelength of 800 nm is cut off from the signals using a notch filter of center notch wavelength 808 nm and FWHM 34 nm (NF808-34, Thorlabs). Since the primary breakup of n-heptane conical sheet is at about 1 mm axial distance (from shadowgraphy), microscopic imaging is recommended [9]. Here, a long-distance microscope (LDM, QM-100, Questar) was equipped with a camera to

capture a $3.28 \times 3.28 \text{ mm}^2$ field of view.

For the same experimental arrangement and flow conditions, a two-color phase Doppler anemometry (PDA) system (Dantec make) was used to measure droplet size and velocity at near field locations. The green (514.5 nm) and blue (488 nm) argon laser beams are utilized for measurements. Each beam diameter is 2.2 mm and beam spacing is 38 mm. Focal lengths of transmission and receiver lenses are 350 mm and 310 mm, respectively. Beam crossing forms a probe volume of $0.148 \times 0.148 \times 3.10 \text{ mm}^3$. The receiver probe was set at $\theta = 70^\circ$ off-axis angle in front scattering mode. It is close to Brewster angle for n-heptane (refractive index, $n = 1.392$). In this way, the effect of trajectory ambiguity can be reduced while collecting reflected and refracted light by the receiver probe. The acquisition was limited by 30 seconds or 1,20,000 droplets to achieve convergent statistics. The measurement was carried out from $Z = 1 \text{ mm}$ downstream of the injector orifice. It is shown in the following discussion that the validation rate close to the orifice is lower because of the presence of non-spherical spray structures and maybe the change in morphology of droplets.

Results and Discussion

The primary atomization of n-heptane hollow cone spray for 0.28 g s^{-1} and 8.1 bar injection pressure was captured using microscopic shadowgraphy technique. Instantaneous shadowgraphy image and averaged image (over 20 images) are shown in Fig. 2. In Fig. 2(a), the perturbations at the liquid-air interface are observed to be grown spatiotemporally from nozzle orifice. This entire event is taking place within short distance. From the averaged image in Fig. 2(b), the measured sheet breakup distance and cone angle are in the order of 1 mm and $\sim 82^\circ$, respectively.

In the beginning, new postprocessing technique that depends on interface and curvature was applied to shadowgraphy data to analyse curvature and so to obtain droplet size. However, for shadowgraphy data, the predicted size was not in good agreement with the measured one. The reason is the presence of blurred regions in shadowgraph image. While removing it by allowing the threshold values, it led to change in morphology of liquid structures. It is recommended to use the laser-induced fluorescent (LIF) technique to analyze near-field coherent regions of liquid spray [8, 9].

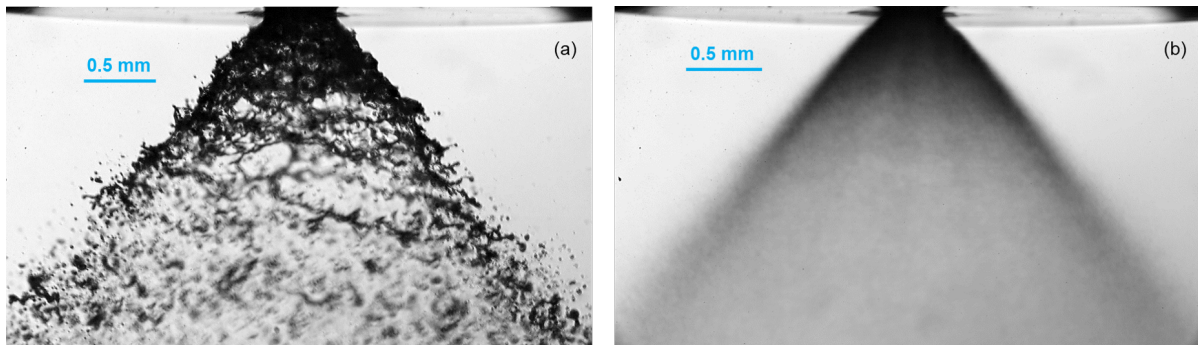


Figure 2. (a) Instantaneous shadowgraph image and (b) averaged image of n-heptane hollow cone spray at 0.28 g s^{-1} and 8.1 bar injection pressure.

Table 1. Solubility test and peak emissions measurement results of various tracer dyes for n-heptane fuel.

Tracer dyes	n-heptane as a solvent	$\lambda_{max,fl}$ at 800 nm	$\lambda_{max,fl}$ at 400 nm	Chemical formula
Fluorescein-548	NO	-	-	$\text{C}_{20}\text{H}_{10}\text{Cl}_2\text{O}_5$
PM-567	YES	576 nm	571 nm	$\text{C}_{22}\text{H}_{33}\text{N}_2\text{BF}_2$
PM-597	YES	592 nm	585 nm	$\text{C}_{20}\text{H}_{33}\text{BF}_2\text{N}_2$
Coumarin-504T	Partial	454 nm	459 nm	$\text{C}_{22}\text{H}_{27}\text{NO}_4$

For LIF, the first challenge was to find a tracer dye for n-heptane fuel. Common tracers for water or amines are fluorescein, eosin, Rhodamine 6G, and many more [8,23]. However, none of these dyes are soluble in nonpolar alkanes like n-heptane. Further, a small number of tracer dyes for n-heptane fuel is noted in the existing literature. There are compromising ways to dissolve polar (eosin) or slightly polar (Nile red) tracer into nonpolar fuel (n-heptane). One of them is by adding a small amount of organic compound (alcohol) into the fuel-tracer solution. Durst et al. [9] added 20% propanol to dissolve eosin Y salt (60 mg l^{-1}) in n-heptane. Adding a small percentage of ethanol into n-heptane and Nile red solution results in a shift of maxima in the emission spectrum [9, 24]. Thus, adding organic compounds can increase the tracer solubility or emission, but it may also change fuel properties. However, this is not the case here, no organic compound was added during the solubility test of various dyes in n-heptane. For solvent n-heptane, the solubility test was performed for the fluorescein-548, pyromethene-597, pyromethene-567, and coumarin-504T. All these dyes are in the solid phase and non-toxic. As expected and explained earlier, fluorescein-548 was found insoluble in n-heptane. Coumarin-504T did not dissolve entirely as some solid particles were observed at the bottom of the solution. However, the other two dyes (pyromethene-567 and -597) were seen to be completely soluble in n-heptane. Table 1 shows the solubility test results. The next step was to achieve the emission spectrum of these dyes with n-heptane.

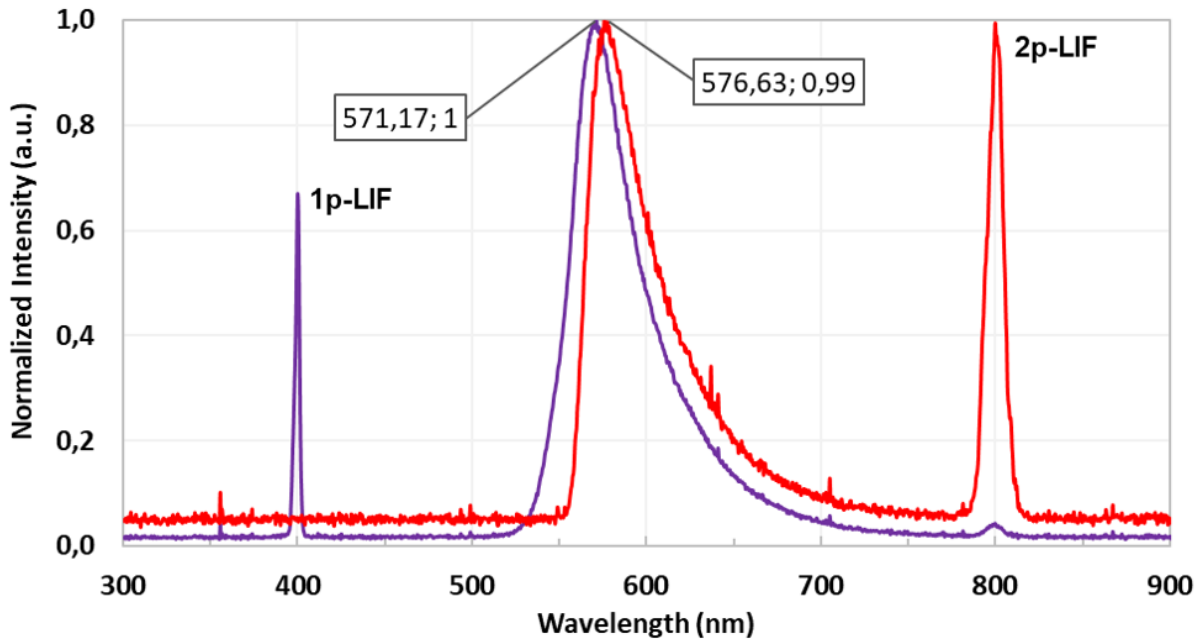


Figure 3. The emission spectrum of n-heptane as fuel and PM-567 as a tracer dye. The violet and red lines corresponds to 1p-LIF and 2p-LIF techniques, respectively. The peak emission of 1p-LIF is $\sim 571 \text{ nm}$, and 2p-LIF is $\sim 576.6 \text{ nm}$ when excited with 400 nm and 800 nm laser light, respectively.

For each tracer dye, a fuel-tracer solution was prepared with 0.5 % by weight dye concentration in n-heptane. The fluoresce characteristic was obtained by measuring emissions when excited with an 800 nm laser light. The peak emission ($\lambda_{max,fl}$) for each solution is tabulated in Table 1. Based on the emission test results and dye concentration, the pyromethene-597 is selected as a tracer dye for n-heptane to perform LIF-based experiments. From now onwards, pyromethene-567 is referred to as PM-567.

The emission spectrum of PM-567 and n-heptane solution for 2p-LIF and 1p-LIF (one-photon laser-induced fluorescent) is shown in Fig. 3. The measured peak emission ($\lambda_{max,fl}$) for 2p-LIF is $\sim 576.6 \text{ nm}$ at peak absorption ($\lambda_{max,abs}$) of 800 nm. Similarly, in the case of 1p-LIF, the peak emission $\sim 571 \text{ nm}$ is noted for 400 nm excitation. The peaks are marked in Fig. 3. The 400 nm laser light was produced by placing a frequency-doubling crystal in an 800 nm laser light path. Both excitation wavelengths (400 nm and 800 nm) are collected directly to show the absorption

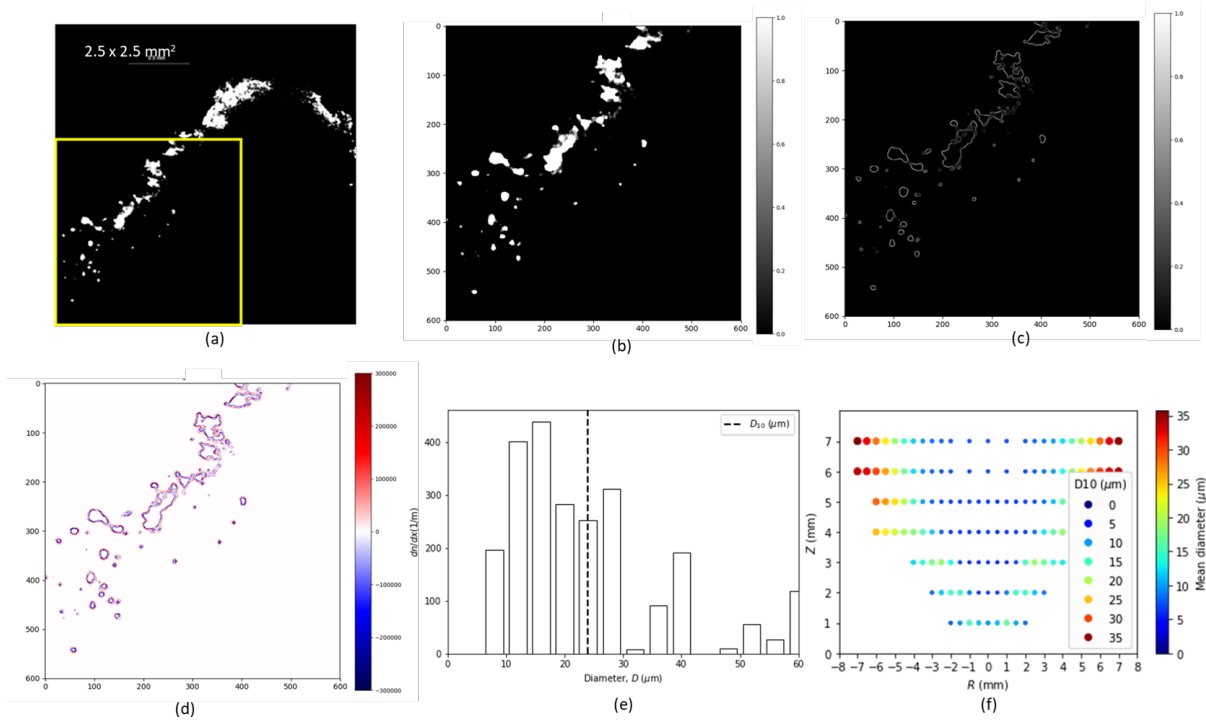


Figure 4. (a) 2p-LIF image of n-heptane hollow cone spray captured at 4.4 fps for 0.28 g s^{-1} mass flow rate and 8.1 bar injection pressure, (b) cropped image, (c) surface interface density Σ , (d) curvature κ ($1/\text{m}$), (e) DSD obtained from interface-curvature analysis and (f) D10 in near-field from PDA measurements.

peak in the spectrum. Considering the advantages of 2p-LIF over 1p-LIF while studying near field regions of optically dense spray [16], the 2p-LIF technique is used in the present work to characterize the initial stage of n-heptane atomization. It provides high-contrast images that facilitate precise curvature information.

N-heptane atomization process at its early stage in the close vicinity of the nozzle is captured using 2p-LIF and processed using interface-curvature analysis proposed by [25] and further developed in [26]. Figure 4 shows the complete analysis and results obtained. In Fig.4(a), 2p-LIF image shows the left part of the spray captured within $2.5 \times 2.5 \text{ mm}^2$. As compared to the shadowgraph image (Fig. 2(a)), the liquid-air interface of liquid structures is easy to trace. Liquid structures that detached from the continuous sheet are considered for the analysis. Thus, the field of view marked by yellow box in Fig. 4(a) and shown in (4(b)) is processed further. A total of 100 images acquired at 4.4 fps were processed in this analysis.

The surface interface density, Σ/Σ_{max} , normalized by maximum is shown in Fig. 4(c). The curvature, $\kappa = \nabla \cdot (\nabla\alpha/|\nabla\alpha|)$ calculated from the surface α is demonstrated in Fig. 4(d). Red and blue color curves in the figure are positive and negative curvatures of the liquid structures, respectively. The droplet size estimated from the curvature is presented by $D_\kappa = 2/\kappa$, and number of droplets by $n_\kappa = S_\kappa/(\pi D_\kappa^2)$. Here S_κ is a total surface interface. Further details about the interface analysis can be seen in [26]. The size distribution of estimated droplets estimated from the interface-curvature analysis is shown in 4(e). The mean diameter D_{10} from the analysis is in the order of $24 \mu\text{m}$. The droplet of similar size can be seen from $Z = 5 \text{ mm}$ axial distance and at the spray wall in PDA measurements of 4(f). A huge amount of data needs to be processed for close estimation at downstream locations.

Summary

The microscopic shadowgraphy imaging is performed for n-heptane continuous conical sheet and dispersed regions. The continuous phase is used to comprehend some spray characteristics. In the beginning, the contours of continuous and dispersed phases captured in the shadowgraphy are used to predict the size of droplets coming out from the atomizing sheet.

However, the predicted size was not in line with the measured diameter due to the presence of blurred regions. Therefore, the next choice to study such dense spray is LIF based technique. The preliminary experiments regarding the selection of tracer dye for n-heptane are presented. 2p-LIF technique was used to capture the near-field atomization process of PM-567 and n-heptane solution. The interface-curvature analysis for 2p-LIF data is presented and initial results are shown. Further analysis of the massive data set is the next step to get a better approximation.

References

- [1] Crua, C., Heikal, M. R., and Gold, M. R., 2015, "Microscopic Imaging of the Initial Stage of Diesel Spray Formation," *Fuel*, 157, pp. 140–150.
- [2] Linne, M. A., Paciaroni, M., Berrocal, E., and Sedarsky, D., 2009, "Ballistic Imaging of Liquid Breakup Processes in Dense Sprays," *Proc. Combust. Inst.*, 32 II(2), pp. 2147–2161.
- [3] Idlahcen, S., Rozé, C., Méès, L., Girasole, T., and Blaisot, J. B., 2012, *Exp. Fluids*, 52(2), pp. 289–298.
- [4] Idlahcen, S., Blaisot, J.-B., Girasole, T., Rozé, C., and Méès, L., 2008, "Ultra-Fast Time Gated Images of a High Pressure Spray," 14th Int Symp on Applications of Laser Techniques to Fluid Mechanics, Lisbon, Portugal, pp. 7–10.
- [5] Kristensson, E., Berrocal, E., Richter, M., Pettersson, S.-G., and Aldén, M., 2008, High-Speed Structured Planar Laser Illumination for Contrast Improvement of Two-Phase Flow Images.
- [6] Berrocal, E., Kristensson, E., Richter, M., Linne, M., and Aldén, M., 2010, "Multiple Scattering Suppression in Planar Laser Imaging of Dense Sprays by Means of Structured Illumination," *At. Sprays*, 20(2), pp. 133–139.
- [7] Kristensson, E., Berrocal, E., Richter, M., and Aldén, M., 2009, "Ultra-Fast Structured Laser Illumination Planar Imaging (SLIPI) for Single-Shot Imaging of Dense Sprays," 11th Int. Annu. Conf. Liq. At. Spray Syst. 2009, ICLASS 2009, 20(4), pp. 337–343.
- [8] Berrocal, E., Kristensson, E., and Zigan, L., 2018, "Light Sheet Fluorescence Microscopic Imaging for High-Resolution Visualization of Spray Dynamics," *Int. J. Spray Combust. Dyn.*, 10(1), pp. 86–98.
- [9] Durst, A., Wensing, M., and Berrocal, E., 2018, "Light Sheet Fluorescence Microscopic Imaging for the Primary Breakup of Diesel and Gasoline Sprays with Real-World Fuels," *Appl. Opt.*, 57(10), p. 2704.
- [10] Morgan, T., Bothell, J., Burtnett, T., Li, D., Aliseda, A., Machicoane, N., Matusik, K., Morgan, T., Bothell, J., Burtnett, T., Li, D., Heindel, T., Morgan, T. B., Bothell, J. K., Burtnett, T. J., Li, D., and Heindel, T. J., 2020, "Optimization of High-Speed White Beam X-Ray Imaging for Spray Characterization."
- [11] Wang, Y., Liu, X., Im, K. S., Lee, W. K., Wang, J., Fezzaa, K., Hung, D. L. S., and Winkelmann, J. R., 2008, "Ultrafast X-Ray Study of Dense-Liquid-Jet Flow Dynamics Using Structure-Tracking Velocimetry," *Nat. Phys.*, 4(4), pp. 305–309.
- [12] Zhang, X., Moon, S., Gao, J., Dufresne, E. M., Fezzaa, K., and Wang, J., 2016, "Experimental Study on the Effect of Nozzle Hole-to-Hole Angle on the near-Field Spray of Diesel Injector Using Fast X-Ray Phase-Contrast Imaging," *Fuel*, 185, pp. 142–150.
- [13] Fansler, T. D., and Parrish, S. E., 2015, "Spray Measurement Technology: A Review," *Meas. Sci. Technol.*, 26(1).
- [14] Linne, M., 2013, "Imaging in the Optically Dense Regions of a Spray: A Review of Developing Techniques," *Prog. Energy Combust. Sci.*, 39(5), pp. 403–440.
- [15] Coghe, A., and Cossali, G. E., 2012, "Quantitative Optical Techniques for Dense Sprays Investigation: A Survey," *Opt. Lasers Eng.*, 50(1), pp. 46–56.
- [16] Berrocal, E., Conrad, C., Püls, J., Arnold, C. L., Wensing, M., Linne, M., and Miranda, M., 2019, "Two-Photon Fluorescence Laser Sheet Imaging for High Contrast Visualization of

- Atomizing Sprays,” OSA Contin., 2(3), p. 983.
- [17] Pawlicki, M., Collins, H. A., Denning, R. G., and Anderson, H. L., 2009, “Two-Photon Absorption and the Design of Two-Photon Dyes,” *Angew. Chemie - Int. Ed.*, 48(18), pp. 3244–3266.
- [18] So, P. T. C., Dong, C. Y., Masters, B. R., and Berland, K. M., 2000, “Two-Photon Excitation Fluorescence Microscopy,” *Annu. Rev. Biomed. Eng.*, 2(1), pp. 399–429.
- [19] Ulrich, H., Lehnert, B., Guénot, D., Svendsen, K., Lundh, O., Will, S., Wensing, M., Berrocal, E., and Zigan, L., 2021, “Analysis of Liquid Spray Structures Using Two-Photon Fluorescence Laser Sheet Imaging,” *Int. Conf. Liq. At. Spray Syst.*, 1(1).
- [20] Guénot, D., Svendsen, K., Björklund Svensson, J., Ekerfelt, H., Persson, A., Lundh, O., and Berrocal, E., 2020, “Simultaneous Laser-Driven x-Ray and Two-Photon Fluorescence Imaging of Atomizing Sprays,” *Optica*, 7(2), p. 131.
- [21] Cordier, M., Vandel, A., Cabot, G., Renou, B., and Boukhalfa, A. M., 2013, “Laser-Induced Spark Ignition of Premixed Confined Swirled Flames,” *Combust. Sci. Technol.*, 185(3), pp. 379–407.
- [22] Verdier, A., Marrero Santiago, J., Vandel, A., Godard, G., Cabot, G., and Renou, B., 2018, “Local Extinction Mechanisms Analysis of Spray Jet Flame Using High Speed Diagnostics,” *Combust. Flame*, 193, pp. 440–452.
- [23] Storch, M., Mishra, Y. N., Koegl, M., Kristensson, E., Will, S., Zigan, L., and Berrocal, E., 2016, “Two-Phase SLIPI for Instantaneous LIF and Mie Imaging of Transient Fuel Sprays,” *Opt. Lett.*, 41(23), p. 5422.
- [24] Greenspan, P., and Fowler, S. D., 1985, “Spectrofluorometric Studies of the Lipid Probe, Nile Red,” *J. Lipid Res.*, 26(7), pp. 781–789.
- [25] Palanti, L., Puggelli, S., Langone, L., Andreini, A., Reveillon, J., Duret, B., Demoulin, F.X., 2021, *International Journal of Multiphase Flows*, 147.
- [26] Ferrando, D., Palanti, L., Demoulin, F.-X., Duret, B., Reveillon, J., Aug. 29 - Sept 2. 2021, 15th Triennial International Conference on Liquid Atomization and Spray Systems.